equilibration after the beginning of the reaction.

In contrast with the results obtained for $[Ni(cyclam)]^{2+}$,[2] the formation of binuclear $[Ni_2(L)_2ox]^{2+}$ (L = cyclen and Me_2cyclen) complexes in water solution has not been detected, under the experimental conditions employed, although these complexes have been isolated as crystalline compounds from aqueous solutions. The free energy changes for the reaction of $[Ni(cyclen)]^{2+}$ and $[Ni(Me_2cyclen)]^{2+}$ with the oxalate anion are equal, within experimental error, and are somewhat smaller than that observed for the analogous *cis*-diaquonickel(II) complex of cyclam (Table VIII). The equilibrium constant for the reaction [Ni(cyclam)ox] + $[Ni(cyclam)]^{2+}$ = $[Ni_2(cyclam)_2ox]^{2+}$ is very small (log K = 1.6),[2] and even lower values could be expected for the analogous reactions involving the two 12-membered tetraazamacrocycles. So, $[Ni_2(cyclen)_2ox]^{2+}$ and $[Ni_2(Me_2cyclen)_2ox]^{2+}$ could be formed in solution, though in undetectable concentrations.

As shown in Table VIII, the reactions of oxalate ion with the *cis*-diaquo complexes are exothermic. Both enthalpy and entropy changes contribute similarly to the formation of [Ni(Me_2-cyclen)ox], while the formation of [Ni(cyclen)ox] and [Ni(cyclam)ox] present mainly an entropic nature. In the case of [Ni(Me_2cyclen)ox] the greatest enthalpy and lowest entropy changes are observed. This can be explained by means of solvation effects. As shown by the molecular structures of both 12-membered macrocyclic complexes herein reported, the substituents (hydrogens or methyl groups) on the nitrogen atoms point toward the same side of the macrocyclic ring. Therefore, a different solvation in $[Ni(cyclen)]^{2+}$ and $[Ni(Me_2cyclen)]^{2+}$ in solution is to be expected. The presence of the methyl substituents will reduce the formation of hydrogen bonds between the nitrogen atoms of the ligand, the coordinated water molecules, and the solvent, yielding then a smaller desolvation on coordination of the oxalate ion.

Different thermodynamic behaviors can be observed for the addition of ox^{2-} to the three $[Ni(cyclam)]^{2+}$ complexes in solution. The right disposition of the cis complex for the coordination of ox^{2-} (Chart I) is revealed by the greater free energy change, which is due to both favorable enthalpic and entropic contributions. In contrast, the spontaneity of the addition of the bidentate oxalato ligand to the *trans*-diaquo isomer is only due to the entropy change, as this reaction is almost athermic. The heat evolved in the substitution of the two water molecules by the oxalate ion is counterbalanced by that required for the complex to reach the folded conformation. The highest enthalpy term is observed for the coordination of ox^{2-} to the square $[Ni(cyclam)]^{2+}$ complex, which does not require heat absorption for the detachment of coordinated water molecules. On the other hand, the reduction in the number of molecules occurring in this reaction gives rise to an unfavorable entropic contribution.

All the entropic contributions derived from the different forms compensate between them in such a way that the resulting entropic term for the addition of oxalate to the mixture of $[Ni(cyclam)]^{2+}$ in solution is negligible.

Acknowledgment. This work was partially supported by the Spanish Comisiôn Interministerial de Ciencia y Tecnologia (Proyecto PB85-0190) and the Italian Ministero della Pubblica Istruzione. We are indebted to Dr. Andrea Caneschi for magnetic data collection.

Supplementary Material Available: Listings of crystallographic parameters (Table S1), anisotropic thermal parameters (Tables S2 and S3), hydrogen coordinates (Tables S4 and S5), and nonessential bond angles and distances (Tables S6 and S7) (9 pages); listings of calculated and observed structure factors (Tables S8 and S9) (34 pages). Magnetic data are available on request from the authors. Ordering information is given on any current masthead page.

Contribution No. 5012 from E. I. du Pont de Nemours & Company, Central Research & Development Department, Experimental Station, P.O. Box 80328, Wilmington, Delaware 19880-0328

Electronic and Molecular Structure of $[FKrNCH]^+$. The Question of Hypervalent Bonding

David A. Dixon* and Anthony J. Arduengo, III

Received February 22, 1989

The molecular structure of $[KrFNCH]^+$ has been calculated by using ab initio molecular orbital theory. The force field was calculated, and the molecule is predicted to be linear. Reasonable agreement with the two observed vibrational Raman bands in the solid is found. The stretching mode leading to dissociation into $[KrF]^+$ and NCH is calculated to be near 200 cm^{-1}. The $[KrF]^+$ and NCH fragments in the complex have geometries similar to those for the isolated molecules. The Kr—N bond distance is predicted to be quite short, 2.32 Å. The complex $[FKrNCH]^+$ is predicted to be bound by 38.6 kcal/mol with respect to $[KrF]^+$ and NCH at the MP-2 level (30.2 kcal/mol, SCF level) with zero-point energy corrections. This is much higher than the 16.6 kcal/mol found at the SCF level for the Rb^+ complex with NCH, which corresponds to a purely ionic complex. All of the calculated results are consistent with an ionic and a covalent component in the bonding of $[FKr]^+$ with NCH. The molecular orbitals and bonding are analyzed in terms of three-center and four-center hypervalent bonds. Both types of hypervalent bonds are expected to play a role in the description of the covalent σ-bonding in $[FKrNCH]^+$. The charge distribution for $[FKrNCH]^+$ shows some transfer of electronic charge from the carbon to the $[KrF]^+$ region, consistent with some contribution from the resonance structure F—Kr—N=C^+—H.

Introduction

The electronic and molecular structures of "hypervalent" molecules are of continual fascination to chemists. Molecules that in a formal sense appear to violate the Lewis octet rule are intriguing and help to provide us with new insights into molecular structure and behavior. This is especially true when the atom involved as the hypervalent center is an atom from the first row of the periodic table (n = 2).[1] The presence of the hypervalent bond, the three-center, four-electron (3c,4e) bond, has been used to explain the chemistry and bonding in a wide range of molecules.[2,5] We have recently shown the presence of a 5c,6e hypervalent bond in $[F_f\text{–}I\text{–}F\text{–}I\text{–}R_f]^{-1}$ complexes using a combination of experimental and theoretical techniques.[6] We have extended

(1) (a) Ault, B. S.; Andrews, L. *J. Am. Chem. Soc.* **1976**, *98*, 1591; *Inorg. Chem.* **1977**, *16*, 2024. (b) Lee, D. Y.; Martin, J. C. *J. Am. Chem. Soc.* **1984**, *106*, 5745. (c) Forbus, T. R., Jr.; Martin J. C. *J. Am. Chem. Soc.* **1979**, *101*, 5057.

(2) Musher, J. I. *Angew. Chem., Int. Ed. Engl.* **1969**, *8*, 54. Musher describes the hypervalent bond, the 3c,4e bond, in a valence-bond description based on the models of Pimentel[3] and Rundle.[4]

(3) Pimentel, G. C. *J. Chem. Phys.* **1951**, *19*, 446.

(4) Rundle, R. E. *Surv. Prog. Chem.* **1963**, *1*, 81.

(5) Cahill, P. A.; Dykstra, C. E.; Martin, J. C. *J. Am. Chem. Soc.* **1985**, *107*, 6359. These authors describe the hypervalent bond in simple molecular orbital terms following Musher's[2] valence-bond description.

0020-1669/90/1329-0970$02.50/0

Table I. Bond Distances (Å) for Optimized Geometries

molecule	r(C—H)	r(C≡N)	r(Kr—F)	r(M+—N)	ref
[Kr—F]+			1.697		a
			1.752		24
HC≡N	1.057	1.126			a
	1.064	1.156			23
[F—Kr—N≡CH]+	1.065	1.122	1.709	2.320	a
	1.068	1.128	1.748	2.307	11
	1.067	1.168	1.707	2.313	10
	1.073	1.129	1.772	2.183	10
	1.076	1.175	1.83	2.281	9
[Rb··N≡CH]+	1.061	1.125		2.942	a
[Li··N≡CH]+	1.064	1.123		1.945	a

[a] This work.

our study of the 5c,6e bond to the well-known ion $[Xe_2F_3]^+$.[7] We now wish to explore other types of hypervalent bonds. Schrobilgen[8] recently synthesized [FKrNCH]+ (**1**) and characterized it by NMR and Raman measurements. We were intrigued by the conclusion reached from the experimental work that **1** has the first Kr–N bond. Since this structure is reminiscent of our previous work on 5c,6e bonds, we have calculated the electronic structure of **1** using ab initio molecular orbital theory. In order to model the effects of binding an ion, we have studied the complexes of HCN with Li^+ and Rb^+. Subsequent to the completion and submission of our work,[9-11] three other theoretical studies have appeared in the literature.

Calculations

The calculations were done with the program GRADSCF[12] on a CRAY X-MP/24 computer. Geometries were gradient optimized[13] in $C_{\infty v}$ symmetry at the SCF level. Force fields and infrared intensities were calculated analytically by using the rapid second-derivative methods[14] in GRADSCF. Correlation energy corrections were done at the MP-2 level.[15] Further analysis of the wave function including the calculation of Boys localized molecular orbitals[16] was done with the program GAMESS[17] on the above computer system. The basis set for C, N, and F is the Dunning[18] [5s3p] set augmented by a pair of d functions each of which are formed by a two-term Slater fit[19] with tight exponents of $\zeta_{STO}(F) = 2.2$, $\zeta_{STO}(N) = 2.1$, and $\zeta(C) = 2.0$ with a diffuse exponent for all three of $\zeta_{STO} = 0.7$. The basis set for H is Dunning's triple-ζ set augmented by a p polarization function of exponent 1.0. The krypton basis set is derived from Dunning's[20] (14s11p5d) primitive set augmented by two diffuse d functions of exponents 0.513 and 0.176. The basis is contracted as follows: the first five s orbitals, the first four p orbitals, and the first four d orbitals, are each contracted to a single function; the remaining orbitals are freely varying. For Li^+, the [5s2p1d] contracted set used previously by us in other Li^+-binding studies[21] was employed. For Rb^+, we started with the (17s11p6d) basis set of Huzinaga.[22] To this basis set we added a p-orbital set with exponent 0.0734 and a d-orbital set with exponent 0.3297. Due to linear-dependency problems (we use a six-term d function), the s exponent of 3.9462 was deleted. The orbitals were contracted as follows: the first seven s, the first five p, and the first four d were contracted to a single function; the remaining functions are freely varying. Final contracted basis sets were as follows: F, C, and N, [5s3p2d]; H, [3s1p]; Kr, [9s8p4d]; Li, [5s2p1d]; Rb, [10s8p4d].

Results

Geometry. The optimized geometry parameters for [FKrNCH]+ are given in Table I together with the parameters for KrF^+, HCN, [Li—NCH]+, and [RbNCH]+. Only the geometry of HCN is known from experiment.[23] With this basis set, the value for r(C—H) is calculated to be 0.007 Å less than the experimental value whereas the value for r(C≡N) is calculated to be 0.03 Å too short. For $[KrF]^+$, our calculated value is 0.02 Å longer for r(Kr—F) at the SCF level as compared to Liu and Schaefer's calculated value.[24] Inclusion of electron correlation with a first-order wave function by Liu and Schaefer yielded a value of 1.752 Å for r(Kr—F). Thus our value is ~0.05 Å too short as compared to Liu and Schaefer's correlated value.[25]

For [FKrNCH]+, the CN distance shortens by 0.004 Å whereas r[Kr–F] increases by 0.012 Å. Formation of the complex leads to only small changes in bond distances in the two fragments. The value for r[Kr–N] is quite short, 2.320 Å, and is similar to our calculated value $r(I-F_c)$ in $[FIF_cIF]^{-1}$[3] or to $r(Xe-F_c)$ in $[FXeF_cXeF]^+$.[7] In order to better model this system, we calculated the structure of [RbNCH]+. The ion Rb^+ should be of similar size as compared to "Kr^+" and provides a model for the ionic component of the bond in [FKrNCH]+. The value for r(Rb–N) is 2.942 Å, 0.6 Å longer than r(Kr–N) in [FKrNCH]+. As discussed below, there is little charge transfer from Rb^+ to NCH. Thus the large difference in bond lengths is consistent with some form of chemical bonding in [FKrNCH]+. As expected, the geometry for HCN in [RbNCH]+ is essentially unchanged. Binding Li^+ should produce a tighter ionic interaction, and, indeed, r(Li–N) is only 1.945 Å.

The structures calculated by other workers are also given in Table I. Both structures reported at the Hartree–Fock level show a difference in one bond length in comparison with our results. The structure calculated by Koch[10] has a significantly longer C≡N bond (0.046 Å) whereas the structure determined by MacDougall et al.[11] has a longer Kr—F bond (0.041 Å). Inclusion of correlation effects at the MP-2 level exhibits interesting effects, although the two calculations[9,10] do not agree as well as would be expected. For example, Koch[10] finds a short C≡N bond whereas Hillier and Vincent[9] find a long C≡N bond. Similarly, Hillier and Vincent[9] find a rather long N—Kr bond, which is only 0.04 Å less than our Hartree–Fock value, whereas Koch[10] finds a shortening of 0.13 Å. Both calculations show an increase in the Kr—F bond length with the inclusion of correlation, with Hillier and Vincent[9] finding the largest increase. The general result from the MP-2 studies is a decrease in r(Kr—N) on formation of the complex and an increase in r(Kr—F).

Vibrational Spectra. The calculated frequencies are given in Table II. For HCN, the experimental frequencies are well-

(6) Farnham, W. B.; Dixonn, D. A.; Calabrese, J. C. *J. Am. Chem. Soc.* **1988**, *110*, 8453.
(7) Dixon, D. A.; Arduengo, A. J., III; Farnham, W. B. *Inorg. Chem.* **1989**, *28*, 4589.
(8) Schrobilgen, G. J. *J. Chem. Soc., Chem. Commun.* **1988**, 863.
(9) Hillier, I. H.; Vincent, M. A. *J. Chem. Soc., Chem. Commun.* **1989**, 30.
(10) Koch, W. *J. Chem. Soc., Chem. Commun.* **1989**, 215. We note the possibility of a typographical error in that the SCF and MP-2 values for r(C≡N) may be reversed.
(11) MacDougall, P. J.; Schrobilgen, G. J.; Bader, R. F. W. *Inorg. Chem.* **1989**, *28*, 963.
(12) GRADSCF is an ab initio gradient program system designed and written by A. Komornicki at Polyatomics Research.
(13) (a) Komornicki, A.; Ishida, K.; Morokuma, K.; Ditchfield, R.; Conrad, M. *Chem. Phys. Lett.* **1977**, *45*, 595. McIver, J. W., Jr.; Komornicki, A. *Ibid.* **1971**, *10*, 303. (b) Pulay, P. In *Applications of Electronic Structure Theory*; Schaefer, H. F., III, Ed.; Plenum: New York, 1977; p 153.
(14) King, H. F.; Komornicki, A. In *Geometrical Derivatives of Energy Surface and Molecular Properties*; Jorgenson, P., Simons, J., Eds.; NATO ASI Series C, Vol. 166; D. Reidel: Dordrecht, The Netherlands, 1986; p 207. King, H. F.; Komornicki, A. *J. Chem. Phys.* **1986**, *84*, 5645.
(15) (a) Moeller, C.; Plesset, M. S. *Phys. Rev.* **1934**, *46*, 618. (b) Pople, J. A.; Binkley, J. S.; Seeger, R. *Int. J. Quantum Chem., Symp.* **1976**, *10*, 1.
(16) Boys, S. F. In *Quantum Theory of Atoms, Molecules and the Solid State*; Löwdin, P.-O., Ed.; Academic Press: New York, NY, 1966; p 253. (b) Kleier, D. A.; Halgren, T. A.; Hall, J. H., Jr.; Lipscomb, W. N. *J. Chem. Phys.* **1974**, *61*, 3905.
(17) GAMESS program system from M. Schmidt, North Dakota State University, and S. Elbert, Iowa State University, based on the original program from NRCC by M. Dupuis, D. Spangler, and J. J. Wendoloski, *National Resource for Computation in Chemistry Software Catalog*, Vol. 1, program QG01, Lawrence Berkeley Laboratory, USDOE, Berkeley, CA, 1980. See also: Dupuis, M.; Rys., J.; King, H. F. *J. Chem. Phys.* **1976**, *65*, 111.
(18) Dunning, T. H., Jr. *J. Chem. Phys.* **1971**, *55*, 716.
(19) Stewart, R. F. *J. Chem. Phys.* **1969**, *50*, 2485.
(20) Dunning, T. H., Jr. *J. Chem. Phys.* **1977**, *66*, 1382.
(21) Dixon, D. A.; Gole, J. L.; Komornicki, A. *J. Phys. Chem.* **1988**, *92*, 1378.
(22) Huzinaga, S. *J. Chem. Phys.* **1977**, *66*, 4245.
(23) Harmony, M. D.; Laurie, V. W.; Kuczkowski, R. L.; Schwendeman, R. H.; Ramsay, D. A.; Lovas, F. J.; Lafferty, W. J.; Maki, A. G. *J. Phys. Chem. Ref. Data* **1979**, *8*, 619.
(24) Liu, B.; Schaefer, H. F., III. *J. Chem. Phys.* **1971**, *55*, 2369.
(25) We optimized the bond distance for [KrF]+ at the MP-2 level and obtained a value of 1.748 Å, in excellent agreement with the value of 1.752 Å found by Liu and Schaefer.[24]

Table II. Calculated Molecular Frequencies (cm^{-1}) and Infrared Intensities (km/mol)

mode	ν(calc)[a]	scale factor	ν(expt)	I(calc)[a]
HCN and $[Kr-F]^+$				
C—H	3618	0.915	3311[b]	71
C≡N	2413	0.870	2097[b]	10
H—C≡N (π)	876	0.812	712[b]	70
$[Kr-F]^+$	787	0.793	624[c]	0.3

	ν(calc) HF[a]	ν(scaled) HF[a]	ν(calc) HF[d]	ν(calc) MP-2[d]	ν(calc) MP-2[e]	ν(expt)[h]	I(calc)[a]
			$[F-Kr-N\equiv C-H]^+$				
C—H	3556	3253[f]	3588	3467	3446		133
C≡N	2446	2128[f]	2461	2130	2100	2158	221
H—C≡N (π)	935	760[f]	940	762	752		43
Kr—F	782	620[f]	782	644	562	560	66
bend A (π)	253	228[f]	256	271	244		63
$[FKr]^+$—[HCN] str	217	195[g]	222	287	267		72
bend B (π)	115	104[g]	120	116	117		28
			$[Li-N\equiv C-H]^+$				
Li^+—[HCN]	503	453[g]					141
bend (π)	206	185[g]					232
			$[Rb-N\equiv C-H]^+$				
C—H	3583	3278[f]					96
C≡N	2423	2108[f]					62
H—C≡N (π)	929	754[f]					56
Rb^+—[HCN]	145	130[g]					7.7
bend (π)	133	120[g]					98

[a] This work. [b] Reference 26. [c] Reference 28. [d] Reference 10. [e] Reference 9. [f] Scaled with above scale factors. [g] Scaled with scale factor = 0.9. [h] Reference 8.

known.[26] The calculated frequencies are too high, as would be expected, since we have neglected correlation corrections and anharmonicity.[27] We have calculated scale factors to provide a comparison with the experimental measurements for $[FKrNCH]^+$. Usually the scale factors are ~0.9,[27] as found here for the C–H stretch, but the bend in HCN and the KrF stretch require scale factors of ~0.8. For KrF^+, Liu and Schaefer[24] calculate a value of 621 cm^{-1} at the correlated level, in excellent agreement with the solid-state experimental values of 624 and 619 cm^{-1}.[28]

For $[FKrHCN]^+$, the calculated force field shows the $C_{\infty v}$ symmetry structure to be a true minimum on the potential energy surface. We employ the scale factors calculated above to scale the four highest frequencies. For the three lowest frequencies, we employ the usual scaling factor of 0.9. The calculated frequencies show a decrease in the C–H stretch of ~60 cm^{-1} and an increase in the CN stretch of ~30 cm^{-1}. The degenerate bend involving the HCN moiety shows an increase of ~50 cm^{-1}. Considering the change in the HCN frequencies, we calculate the frequency for the Kr–F fragment to be essentially invariant on formation of the complex. The $[FKr]^+$–[NCH] stretch is quite low, ~200 cm^{-1}, but is still large enough to correspond to a significantly bound complex. The two bends

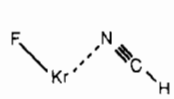

A

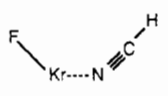

B

are significantly different in frequency, with B the lower energy bend.

The only observed bands in the Raman spectrum attributable to the complex are an intense band at 560 cm^{-1} and a band at 2158 cm^{-1}. The observed shift to higher frequency for the CN stretch is consistent with our calculated shift, especially when it is noted that the shift is 42 cm^{-1} above the unreacted CN band. The calculated shift is 32 cm^{-1}. Our calculated value for the Kr–F stretch is not consistent with the observed large shift to lower frequency. As discussed below, this could be due to a very large correlation effect on this quantity.

The vibrational spectra for the Rb^+ and Li^+ complexes show effects similar to those observed in complexing $[KrF]^+$. The CH frequencies decrease in the complex and the CN frequencies increase when compared to those in HCN. As expected, the smallest effects are observed for Rb^+ binding. The HCN bend also increases on binding Rb^+ and Li^+, just as found in binding KrF^+, with Li^+ having the largest effect. Binding of Rb^+ leads to a much lower stretching frequency for the M^+–N bond as compared to $[Kr-F]^+$ binding, consistent with the long Rb^+–N bond length. The value for the Li^+–N stretch is much higher, consistent with the lighter mass of Li^+ and the shorter Li^+–N bond length.

We compare our calculated frequencies to those calculated by Koch[10] and by Hillier and Vincent[9] in Table II. The Hartree–Fock frequencies of Koch are in good agreement with our values. The frequencies calculated at the MP-2 level are lower than our values, as would be expected. The CN stretch in HCN is calculated to be too low (2038 cm^{-1}) at the MP-2 level.[29] We thus expect the calculated CN stretch in **1** to also be too low. A similar result is found for the bend in HCN where the MP-2 value[29] (707 cm^{-1}) is also less than the experimental value. The major differences between the MP-2 and Hartree–Fock values are for the Kr–F and $[FKr]^+$–NCH stretches, consistent with these bond distances showing the largest effect of electron correlation. The calculated Kr–F stretch in **1** shows a larger correlation correction than found for $[Kr-F]^+$. Due to the calculated differences in the Kr–F bond lengths in **1**, the two MP-2 calculations give quite different Kr–F frequencies. Since anharmonicity corrections are not expected to be negligible, the value of Hillier and Vincent[9] seems to be quite low, as their harmonic value is essentially the experimental value. Both MP-2 calculations give significantly stronger $[F-Kr]^+$–NCH bond stretches, consistent with the shorter Kr–N bond distances. This is also consistent with the energy results quoted below which

(26) Herzberg, G. *Electronic Spectra and Electronic Structure of Polyatomic Molecules*; Van Nostrand Reinhold Co.: New York, 1966.
(27) Dixon, D. A. *J. Phys. Chem.* **1988**, *92*, 86.
(28) Gillespie, R. J.; Schrobilgen, G. J. *Inorg. Chem.* **1976**, *15*, 22.
(29) Hehre, W. J.; Radom, L.; Schleyer, P. V. R.; Pople, J. A. *Ab Initio Molecular Orbital Theory*; Wiley-Interscience: New York, 1986; p 239.

Table III. Total Energies (au)

molecule	SCF	MP-2
Li^+	-7.236 211	
Rb^+	-2937.495 738	
HCN	-92.908 576	-93.210 314
$[KrF]^+$	-2850.875 320	-2851.215 196
$[FKrNCH]^+$	-2943.834 060	-2944.489 138
$[LiNCH]^+$	-100.202 363	-100.501 237
$[RbNCH]^+$	-3030.675 160	

Table IV. Binding Energies (kcal/mol)

molecule	ΔE(SCF)	ΔE(MP-2)	ΔH(0 K)
$[FKr]^+\cdots NCH$	31.5	39.9	38.6
$Rb^+\cdots NCH$	17.2		16.6
$Li^+\cdots NCH$	36.1	34.3	33.0

Table V. Molecular Charges (e)

molecule	H	C	N	M	E
$[Kr-F]^+$				+1.15	-0.15
HC≡N	+0.24	-0.04	-0.20		
$[F-Kr\cdots N\equiv CH]^+$	+0.31	+0.21	-0.23	+1.00	-0.29
$[Rb\cdots N\equiv CH]^+$	+0.28	+0.07	-0.34	+1.00	
$[Li\cdots N\equiv CH]^+$	+0.31	+0.18	-0.26	+0.77	

show a significant correction effect (~20%) on the binding energy of $[Kr-F]^+$ with HCN.

Binding Energies. We have calculated the binding energy of M^+ with HCN just as one calculates the binding energy of a proton, the proton affinity.[30] The total energies are summarized in Table III, and relative energies are given in Table IV. The SCF binding energy is 31.5 kcal/mol for $[Kr-F]^+$ binding to HCN whereas the correlated value at the MP-2 level is 39.9 kcal/mol. These values are in good agreement with those of Koch,[10] who finds ΔE = 31.3 kcal/mol at the SCF level and 41.8 kcal/mol at the MP-2 level, considering the differences in basis sets and geometries. We note that higher orders of correlation (MP-4) do not significantly affect the binding energy.[10] For Li^+ binding to NCH, the interaction energy is 36.1 kcal/mol at the SCF level and 34.3 kcal/mol at the correlated level. The small correlation correction for Li^+ binding is consistent with other studies of the binding of Li^+ to N_2 and CO.[21] We note that the MP-2 level may lead to an overestimate of the correlation effect on binding Li^+ by about 1 kcal/mol, which is not significant here. The binding energy of Rb^+ is only 17.2 kcal/mol at the SCF level, about half the binding energy found for $[Kr-F]^+$. An MP-2 correction for Rb^+ binding could not be obtained due to the near-linear dependency in the basis set noted above. However, the MP-2 correction is expected to be on the order of 1 kcal/mol on the basis of the Li^+ value. The low binding energy for Rb^+ as compared to that of $[Kr-F]^+$ clearly demonstrates that there is significant additional energy in the $[FKr]^+$–NCH interaction beyond that of the ion-dipole type expected for Rb^+ binding. We can thus estimate that the minimum ionic character is 17 kcal/mol and the maximum covalent character is 23 kcal/mol for the $[FKr]^+$–NCH bond. The binding energy of $[Kr-F]^+$ is comparable to that of Li^+ even though Li^+ has a much shorter M^+–N bond distance. The analysis up to this point—geometries, frequencies, and binding energies—clearly points to some sort of chemical bonding phenomena in $[FKrNCH]^+$ in addition to the ion-dipole bonding expected for a sphere of point charge interacting with HCN.

Atomic Populations. The atomic charges (Table V) can be used to estimate the amount of charge transfer between the ion and HCN. $[Kr-F]^+$ has the positive charge localized on Kr, and fluorine has a negative charge of -0.15 e. In HCN the hydrogen is positive and the nitrogen negative with the carbon being essentially neutral. In $[FKrNCH]^+$ there is a significant transfer of electronic charge (0.30 e) from the HCN to the $[KrF]^+$. Most of the charge is transferred from the carbon and is equally shared by the Kr and F. The charge distribution for $[FKrNCH]^+$ is consistent with the resonance structure $F-Kr-N\equiv C^+-H$ having some role. In contrast, there is no transfer of charge to Rb^+ from HCN in $[RbNCH]^+$. Rather, there is a polarization of charge in the CN bond, with the nitrogen increasing its negative charge and the carbon losing negative charge. In the Li^+ complex, negative charge is again transferred from the carbon to the Li^+. The results for the charges are consistent with the above results that showed a chemical bonding interaction in $[FKrNCH]^+$.

Molecular Orbitals. The molecular orbitals for $[Kr-F]^+$ and HCN are summarized in Table VI. The HOMO for $[Kr-F]^+$ is the π^* orbital, mostly localized on Kr, and the NHOMO is the Kr–F σ bond. The third highest occupied MO is the π orbital

Table VI. Orbitals for $[Kr-F]^+$ and HCN

orbital	orbital energy, eV
$[Kr-F]^+$	
HOMO (π^* mostly on Kr)	23.82
NHOMO (Kr–F σ)	28.22
OMO (π, more on F)	28.91
LUMO (Kr–F σ^*)	8.49
HCN	
HOMO (CN π)	13.74
NHOMO (N lp + $\alpha\sigma$(C–N))	15.81
LUMO (HC–N σ^*(s))	-1.32

Table VII. $[F-Kr-N\equiv C-H]^+$ Orbitals

description	energy, eV
π – CN π (very small π^* component on Kr) HOMO	19.81
σ – extended σ--σ_6	22.02
π – Kr–F π^*, mostly on Kr	22.14
π – Kr–F π, mostly on F	26.48
σ – [σ(Kr–F) – σ(C–H) – P_N]--σ_5	26.79
σ – [σ(Kr–F) – σ(C–H) + P_N]--σ_4	27.82
σ – [Kr "s" – σ(C–N)]--σ_3	39.70
σ – [Kr "s" + σ(C–N)]--σ_2	40.50
σ – F "2s"--σ_1	51.35

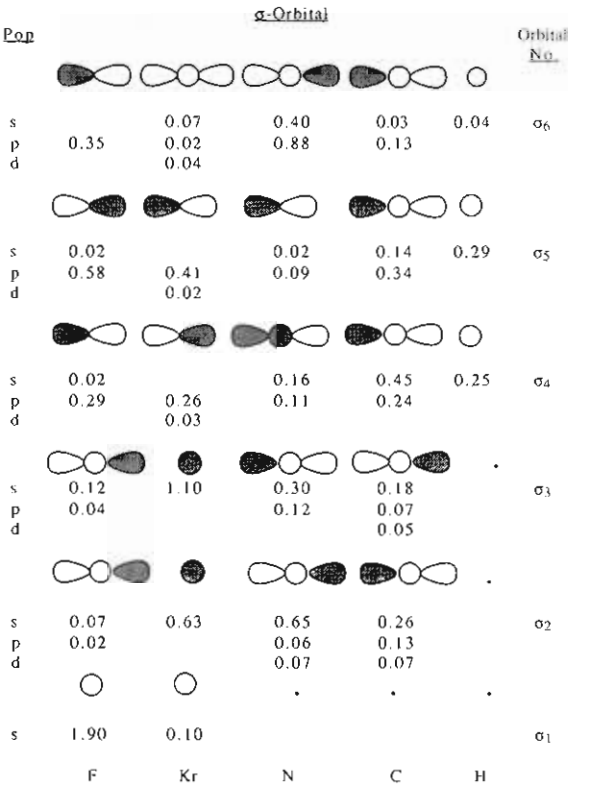

Figure 1. Population analysis of the six σ-bonding orbitals for $[FKrNCH]^+$. The phases are taken from the canonical molecular orbitals.

(30) Dixon, D. A.; Lias, S. G. In *Molecular Structure and Energetics*; Liebman, J. F.; Greenberg, A., Eds.; VCH: Deerfield Beach, FL, 1987; Vol. 2, p 269.

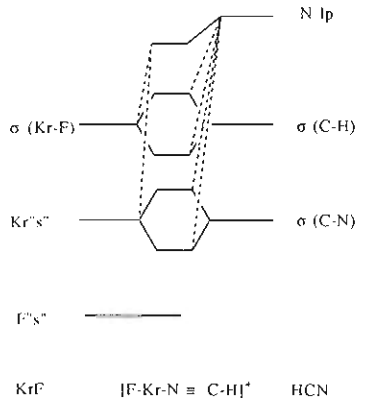

Figure 2. Qualitative molecular orbitals diagram showing which fragment orbitals are coupled to produce the molecular orbitals of the complex. The energy of the orbitals increases from bottom to top.

of the diatomic localized mostly on F. The LUMO, of course, is the Kr–F σ^* orbital. For HCN, the HOMO is the CN π bond, and the NHOMO is a mixture of the lone pair on N and the C–N σ bond. The LUMO for HCN is a σ^* orbital with large s character on H, C, and N.

The above orbitals can be used to construct the molecular orbitals of the complex; these are summarized in Table VII, and a schematic of the σ orbitals is shown in Figure 1. Of the top four orbitals, only the NHOMO is a σ orbital. The three π orbitals are like the π orbitals of the fragments with little delocalization. The NHOMO σ_6 orbital is delocalized over four atomic centers (excluding hydrogen). Most of the density (1.28 e) is on the nitrogen with the next largest density on the terminal fluorine. Kr and C have comparable populations of 0.13 and 0.16 e, respectively. Most of the density is in the p orbitals although the nitrogen has a significant s component. The nodal properties of the NHOMO show bonding between C and N. There is a node in the p orbitals between Kr and N, but the Kr d orbital leads to a bonding interaction between Kr and N. The orbital σ_5 has low density at the nitrogen and is composed of the antibonding combination of the C–H and Kr–F bonds. Orbital σ_4 is the bonding combination of the σ(CH) and Kr–F orbitals. There is more density on the N in σ_4 as compared to σ_5. The nodal properties of σ_4 show a bonding interaction between N and Kr and a node between N and C. Orbital σ_3 has a large population on Kr predominantly in the valence s orbital. The next largest population is found on the nitrogen, followed by carbon and then fluorine. The nodal properties show antibonding behavior in the s orbitals but bonding between the Kr s orbital and the p orbitals on the adjacent centers. Orbital σ_2 has its largest populations on N and Kr; the population on C is also significant. This orbital is predominantly an in-phase combination of s orbitals on Kr, N, and C. The p orbitals between C and N are bonding whereas the p orbital on N is antibonding with respect to the Kr s orbital. The population on F is much smaller. The lowest energy σ orbital, σ_1, is the 2s orbital on F.

The orbital mixings described above are summarized schematically in Figure 2. The lone pair on N is stabilized by mixing with the various σ orbitals and allowing it to delocalize. The remaining σ orbitals are described as the bonding and antibonding mixing of the σ(Kr–F) and the σ(C–H) orbitals, the bonding and antibonding mixing of the Kr valence orbital and the σ(C–N) orbital, and the F 2s orbital.

Localized Molecular Orbitals. The centroids of charge for the localized molecular orbitals are given in Table VIII. The LMO's show three lone pairs on F, three lone pairs on Kr (toward the F), a Kr–F σ bond, three τ bonds between C and N, and a C–H bond. The final LMO is the nitrogen lone pair that is located between N and Kr. The lone pair centroid on N is 1.22 au away from the N as compared to the lone pair in HCN, which is 0.70 au away from the N. Clearly the lone pair on N is more delocalized toward Kr in $[FKrNCH]^+$. Whereas the N lone pair is essentially completely localized on N in HCN, the lone pair

Table VIII. Centroids of Charge for LMO's of $[FKrNCH]^+$

	molecular coordinates, au		
atom	*x*	*y*	*z*
F	−3.604011	0.0	0.0
Kr	−0.374076	0.0	0.0
N	4.010443	0.0	0.0
C	6.130592	0.0	0.0
H	8.142284	0.0	0.0
	centroids, au		
orbitals	*x*	*y*	*z*
N lp	2.79377	0.0	0.0
Kr lp	−0.53203	0.01799	0.89644
Kr lp	−0.53203	−0.78533	−0.43264
Kr lp	−0.53203	0.76734	−0.46380
F lp	−3.96198	−0.28134	−0.41321
F lp	−3.96198	0.49852	−0.03704
F lp	−3.96198	−0.21718	0.45025
Kr–F σ	−2.73486	0.0	0.0
C–N τ	4.59966	−0.04167	−0.57694
C–N τ	4.59966	0.52048	0.25239
C–N τ	4.59966	−0.47881	0.32455
C–H σ	7.07850	0.0	0.0

delocalizes by 0.24 e onto Kr in $[FKrNCH]^+$. The hybridization of the lone pair on N in HCN is $sp^{0.79}$; the p character increases in the complex to give a hybridization of $sp^{0.88}$. The increase in p character is consistent with the shift in the position of the centroid of charge toward Kr and the delocalization onto Kr.

Bonding Models. A schematic of the 3c,4e hypervalent bond is shown as follows:

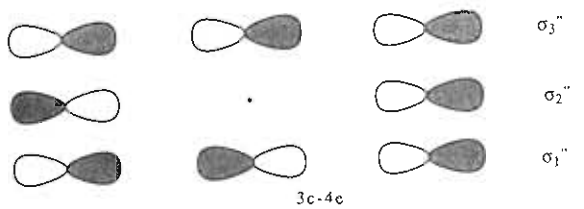

3c-4e

The 3c,4e bond, to a first approximation, can be derived from the π orbitals of the allyl system by rotating the p orbitals into the plane to make σ bonds. A similar model was used to generate the 5c,6e bond by using the pentyl orbitals. All of the above results for $[FKrNCH]^+$ are clearly consistent with some type of covalent bonding. How should we best describe this bonding? One possible model for the hypervalent bond for $[FKrNCH]^+$ would be to extend the bond over four centers, where we exclude the H from contributing.[31] A schematic for such a four-center hypervalent bond is shown as follows:

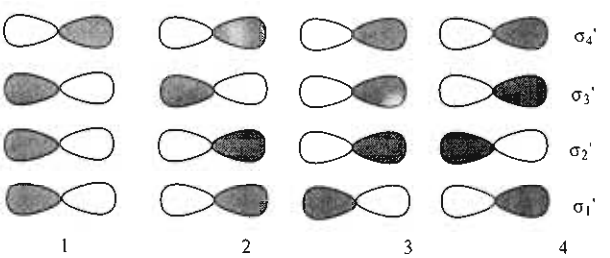

4c

The number of electrons appropriate for this scheme would be either 4 or 6. Orbital σ_1 is clearly bonding in nature. However, orbital σ_2, which will be occupied, has a node between atoms 2 and 3 due to an antibonding interaction between adjacent p orbitals. This is clearly different from the 3c or 5c hypervalent bonds, where the occupied σ obitals have nodes at atoms not

(31) We exclude the C–H bond from contributing to the four-center bond because it is essentially playing the role of a spectator. Since the hydrogen is not directly bonded to the central atoms in the hypervalent bond and only has an s orbital, it will not play an important role in a four-center hypervalent bond composed of p orbitals.

between atoms in bonds.[32] Orbital σ_3 has nodes between atom pairs 1 and 2 and pairs 3 and 4, and the 2-3 interaction is bonding, again different from the 5c scheme. Thus we would expect the 4c hypervalent bond to be significantly weaker than the 3c or 5c hypervalent bonds. In the 4c bond, nodes occur between atoms in the occupied orbitals whereas, in the 3c and 5c bond, nodes occur at atoms in these orbitals.

The above simple model assumes that the atoms are of equal electronegativity. However, in $[FKrNCH]^+$ the atoms are clearly not of equal electronegativity. Furthermore, the C-H bond is of the right energy for mixing, which complicates the analysis. The presence of a triple bond between C and N is also a complicating factor, as this increases the s component (sp hybridization) in the C-N σ bond, which would be part of the 4c hypervalent bond. Examination of Figure 1 shows that the orbitals do not delocalize as extensively as suggested by our model for the 4c hypervalent bond due to the large electronegativity differences. Furthermore, the s and p orbitals are clearly mixed. The highest occupied σ orbital, σ_6, is similar to orbital σ_2' of the 4c bond with the largest population on N and the next highest population on F. Because of the large s character in the CN σ bond, this orbital is very low in energy and the C-H σ bond mixes with the Kr-F σ bond instead of mixing with the C-N σ bond as one would expect from the 4c hypervalent bond. The CN σ bond is mixing, instead, with the Kr valence s orbital. Thus the bonding of the σ_1' orbital of the 4c bond is dispersed over a range of σ orbitals.

Another model for this bonding would involve considering both the C-N and C-H bonds as "spectators" and dealing only with a normal 3c,4e hypervalent bond centered at Kr based on the Kr-F σ bond and the lone pair on N. In this case, σ_6 of $[FKrNCH]^+$ is like σ_2'' of the 3c,4e bond. There is essentially a node at Kr, and the population is not equally distributed between N and F. The σ_4 orbital of the complex then corresponds to σ_1'' of the 3c,4e bond. A complication for this model is that the 3c,4e bond preferentially places the least electronegative atom in the center. Clearly, "Kr^+" is not the least electronegative atom. In order for it to lower its electronegativity in order to participate in the hypervalent bond, charge transfer occurs from the C-H region to the Kr to lower its positive charge and hence its electronegativity. This is actually observed in the population analysis and is consistent with the resonance structure shown above.

All of our results are consistent with some type of covalent bonding interaction in $[FKrNCH]^+$ being present. However, as the above discussion points out, there is no clear choice between the 3c and 4c hypervalent bond models. Rather, the bonding description for the interaction of $[FKr]^+$ with NCH has components of both models present. The results do show that the bonding between Kr and N is not a simple covalent σ bond between two centers but rather is best described in terms of hypervalent bonds.

Registry No. KrFNCH, 118494-40-9.

(32) Arduengo, A. J.; Burgess, E. M. *J. Am. Chem. Soc.* **1977**, *99*, 2376.

Contribution from the Laboratory for Electron Spectroscopy and Surface Analysis, Department of Chemistry, University of Arizona, Tucson, Arizona 85721

Electronic Structure Factors of Si-H Bond Activation by Transition Metals. Valence Photoelectron Spectra of $(\eta^5\text{-}C_5H_4CH_3)Mn(CO)(PMe_3)HSiCl_3$ and $(\eta^5\text{-}C_5H_4CH_3)Mn(CO)(PMe_3)HSiHPh_2$ (Me = CH_3, Ph = C_6H_5)

Dennis L. Lichtenberger* and Anjana Rai-Chaudhuri

Received July 5, 1989

The valence photoelectron spectra of $(\eta^5\text{-}C_5H_4CH_3)Mn(CO)(L)HSiCl_3$ and $(\eta^5\text{-}C_5H_4CH_3)Mn(CO)(L)HSiHPh_2$, where L is CO or $P(CH_3)_3$, are compared to determine the effect of ligand substitution at the metal center on Si-H bond activation. Metal centers that are more electron rich may promote more complete oxidative addition of the Si-H bond to the metal. The shifts in the metal and ligand ionization energies and the relative intensities of ionizations in the He I and He II photoelectron experiments show that the metal in $(\eta^5\text{-}C_5H_4CH_3)Mn(CO)(PMe_3)HSiCl_3$ is best represented by a formal oxidation state of III (d^4 electron count). This indicates nearly complete oxidative addition of the Si-H bond to the metal center and results in independent Mn-H and Mn-Si bonds. In contrast, the splitting and intensity pattern of the metal-based ionizations of $(\eta^5\text{-}C_5H_4CH_3)Mn(CO)(PMe_3)HSiHPh_2$ reflect the formal d^6 electron count of a metal corresponding to oxidation state I. The extent of electron charge density shift from the metal to the ligand is also small, as evidenced by the negligible shifts of these ionizations from those of the related $(\eta^5\text{-}C_5H_4CH_3)Mn(CO)_2(PMe_3)$ complex. These observations indicate that the electronic structure of the Si-H interaction with the metal in this complex is in the initial stages of Si-H bond addition to the metal, before oxidative addition has become prevalent. Comparison with the previously reported photoelectron spectra of $(\eta^5\text{-}C_5H_5)Mn(CO)_2HSiCl_3$ and $(\eta^5\text{-}C_5H_4CH_3)Mn(CO)_2HSiHPh_2$ shows that the Si-H bond interaction with the transition metal is affected more by alkyl and halogen substitutions on silicon than by substitution of a carbonyl with typical two-electron donor ligands at the metal center.

Introduction

Studies of complexes with the general molecular formula $(\eta^5\text{-}C_5R'_5)Mn(CO)(L)HER_3$ (R' = H, CH_3; L = CO, PMe_3; E = Si, Ge, Sn; R = Ph, Cl) have provided a wealth of information on different stages of interaction of an E-H bond with a metal center.[1] In addition to contributing to an understanding of the electronic factors of general E-H bond activation and oxidative addition to a metal center, the complexes are important as models for catalysts in hydrosilation reactions.[2] The X-ray and neutron diffraction structures,[1,3-5] ^{29}Si NMR shifts and couplings,[1] and reaction chemistry[6-8] and rates[9] of these complexes are interpreted in some cases in terms of a three-center-two-electron Mn←H-E

* To whom correspondence should be addressed.

(1) Schubert, U.; Scholz, G.; Muller, J.; Ackermann, K.; Worle, B. *J. Organomet. Chem.* **1986**, *306*, 303 and references therein.
(2) Randolph, C. L.; Wrighton, M. S. *J. Am. Chem. Soc.* **1986**, *108*, 3366.
(3) Schubert, U.; Ackermann, K.; Kraft, G.; Worle, B. *Z. Naturforsch., B* **1983**, *38*, 1488.
(4) Schubert, U.; Ackermann, K.; Worle, B. *J. Am. Chem. Soc.* **1982**, *104*, 7378.
(5) Smith, R. A.; Bennett, M. J. *Acta Crystallogr., Sect. B* **1977**, *B33*, 1113.
(6) Colomer, E.; Corriu, R. J. P.; Marzin, C.; Vioux, A. *Inorg. Chem.* **1982**, *21*, 368.
(7) Colomer, E.; Corriu, R. J. P.; Vioux, A. *Inorg. Chem.* **1979**, *18*, 695.
(8) Jetz, W.; Graham, W. A. G. *Inorg. Chem.* **1971**, *10*, 4.

0020-1669/90/1329-0975$02.50/0